ELSEVIER

Polymer 43 (2002) 7367–7376

polymer

www.elsevier.com/locate/polymer

Super polyolefin blends achieved via dynamic packing injection molding: the morphology and mechanical properties of HDPE/EVA blends

Bing Na, Qin Zhang, Qiang Fu*, Gong Zhang, Kaizi Shen

Department of Polymer Science & Materials, State Key Laboratory of Polymer Materials Engineering, Sichuan University, Chengdu 610065, People's Republic of China

Received 23 May 2002; received in revised form 29 August 2002; accepted 3 September 2002

Abstract

As a part of long-term project aimed at super polyolefin blends, in this work, we report the mechanical reinforcement and phase morphology of the blends of high-density polyethylene (HDPE) and ethylene vinyl acetate (EVA) achieved by dynamic packing injection molding. The shear stress (achieved by dynamic packing injection molding) and interfacial interaction (obtained by using EVA with different VA content) have a great effect on phase morphology and thus mechanical properties. The super HDPE/EVA blends having high modulus (1.9–2.2 GPa), high tensile strength (100–120 MPa) and high impact strength (six times as that of pure HDPE) have been prepared by controlling the phase separation, molecular orientation and crystal morphology of the blends. The phase inversion was also found to shift towards lower EVA content under shear stress. The enhancement of tensile strength and modulus originates from the formation of oriented layer, while the high impact strength is related to shear induced phase morphology. DSC studies indicated that the shish kebab crystal structure that also contributes to the enhancement of tensile strength is formed in the oriented layer. The dramatic improvement of impact strength may result from the formation of microfibers and elongated EVA particles along the flow direction. Wu's toughening theory was found non-applicable for the elongated and oriented rubber particles, and a brittle–ductile–brittle transition was observed with increasing EVA content.

Keywords: High-density polyethylene/ethylene vinyl acetate blends; Shear; Interfacial interaction

1. Introduction

The study on the improvement of mechanical properties in polyolefin is always attracting much attention. Many literatures about increasing the impact strength of polyolefin have been reported extensively [1–5]. By blending them with the rubber particles, the impact strength of polyolefin can be improved significantly. Moreover, various toughening mechanisms and models have been proposed. Several studies have documented the effect of various parameters such as rubber particle size, rubber concentration and interparticle distance on the toughening efficiency of rubber particles [6–8]. Unfortunately, with the increasing of impact strength, the tensile strength as well as modulus always declines. In recent years, many researchers have paid more attention to the preparation of polyolefin with high impact strength, as well as high tensile strength and high modulus, which relies on structure manipulation during melt processing. Allowed for the chain-folded, the high performance can be obtained by the *c*-axis orientation through the stacks of lamellae or the chain-folded blocks with straight stem directions all parallel [9]. In light of this, recent efforts have been directed towards the achievement of high chain extensions in addition to chain orientation.

Tensile drawing [10], die drawing [11], hydrostatic extrusion [12,13], capillary extrusion [14], high-pressure injection molding [15] and shear-controlled orientation in injection molding (SCORIM) [16–18] are the examples that make use of the principle of orientation. It is believed that the more is the degree of orientation, the higher is the strength and modulus (up to 10^{11} N m^{-2} for HDPE [14]). Meanwhile, the improvement of strength and modulus also results from nucleating the lamellae in close proximity to each other along parallel chain aligned fibrous crystals. The fibrous crystals are produced by elongational flow-induced chain extension, and serve merely to set the pattern for the subsequent lamellar crystal growth. In addition, the intimate

* Corresponding author. Fax: +86-28-5405402.
E-mail address: fuqiang1963@yahoo.com (Q. Fu).

0032-3861/02/$ - see front matter
PII: S0032-3861(02)00637-7

interlocking of adjacent row nucleated columns, which is produced by the tapering lamellae due to increasing supercooling which is itself a consequence of the rising hydrostatic pressure during lamellae growth plays a vital role for the high modulus [14].

In our previous papers [19,20], we reported the results of mechanical properties and structural studies of some polyolefin blends (such as HDPE/LDPE, HDPE/iPP, iPP/EPDM) obtained by dynamic packing injection molding. We have found that the molecular architecture, composition, temperature and shear stress field play an important role to determine the final morphology and mechanical properties. It is widely accepted that the morphology resulting from blending and processing depends mainly upon the rheological and interfacial properties, the blending conditions, and the volume ratio of the components [21–24]. In this work, we focus on the effect of volume ratio, shear stress and interfacial interaction on phase morphology. The effect of shear stress was achieved by dynamic packing injection molding, and different interfacial interaction was obtained by using different VA content of EVA. Our proposals are two-folds, one is to better understand the morphological development of polymer blends during external shear stress, and the other is to achieve super polyolefin blends with both high modulus and impact strength by controlling orientation, phase separation and crystal morphology.

2. Experimental

2.1. Materials

The HDPE and EVAs, used in the experiment, are all commercialized products, and summarized in Table 1. Three kinds of EVA were used with VA content 16 wt% (16EVA), 33 wt% (33EVA) and 41 wt% (41EVA). It should be noted that the melt flow index of EVA also increases as increasing of VA content.

2.2. Samples preparation

Melt blending of HDPE/EVA was conducted using twin-screw extruder (TSSJ-25 co-rotating twin-screw extruder) set at a barrel temperature of 160–190 °C. After making droplets, the blends were injected into a mold of 3 mm in thickness and 6 mm in width, using SZ 100 g injection molding machine set at 190 °C and 900 kg cm^{-2}. The maximum shear rate was $1.5 \times 10^4 s^{-1}$. Then dynamic packing injection molding technology was applied, which relies on the application of shear stress fields to melt/solid interfaces during the packing stage by means of hydraulically actuated pistons. The detailed experiment procedures were described in Ref. [19]. The main feature is that after the melt is injected into the mold the specimen is forced to move repeatedly in a chamber by two pistons that move reversibly with the same frequency as the solidification progressively occurs from the mold wall to the molding core part. The processing parameters are listed in Table 2. We also carried out injection molding under static packing by using the same processing parameters but without shearing for comparison purpose. The specimen obtained by dynamic packing injection molding is called dynamic sample, and the specimen obtained by static packing injection molding is called static sample.

Table 1
Material used in the investigation

	Trade name	Characteristics	Producer
HDPE	2200J	MFI = 5.8 $d = 0.968$	Yansan Petrochemical Corporation
16EVA	630	MFI = 15 $d = 0.936$ VA% = 16	Toyo Soda Manufacturing Co. Ltd
33EVA	MB11	MFI = 45 $d = 0.960$ VA% = 33	Sumitomo Chemical Co. Ltd
41EVA	40w	MFI = 65 $d = 0.968$ VA% = 41	Dupont Corporation

2.3. Mechanical properties measurement

Shimadzu AG-10TA Universal Testing Machine was used to measure the stress–strain curves, the moving speed was 50 mm min^{-1}. The measure temperature was 20 °C. For impact strength measurement, the central part of sample (40 mm long) was used. A notch with 45° was made by machine and remained width is 5.0 mm. The experiment was carried out on an I200XJU-2.75 Impact tester according to ISO 179. Since the specimen is not standard, the notched impact strength only can be used as a comparison value, and the relative impact strength was used in the data treatment. The values of all the mechanical parameters are calculated as averages over six to nine specimens for each composition.

Table 2
Processing parameters in oscillating packing injection molding of HDPE/EVA blends

Parameters	Values
Injection pressure	90 MPa
Oscillating packing pressure	4 MPa
Oscillating frequency	0.3 Hz
Holding time	2 min
Melt temperature	180 °C
Mold temperature	40 °C

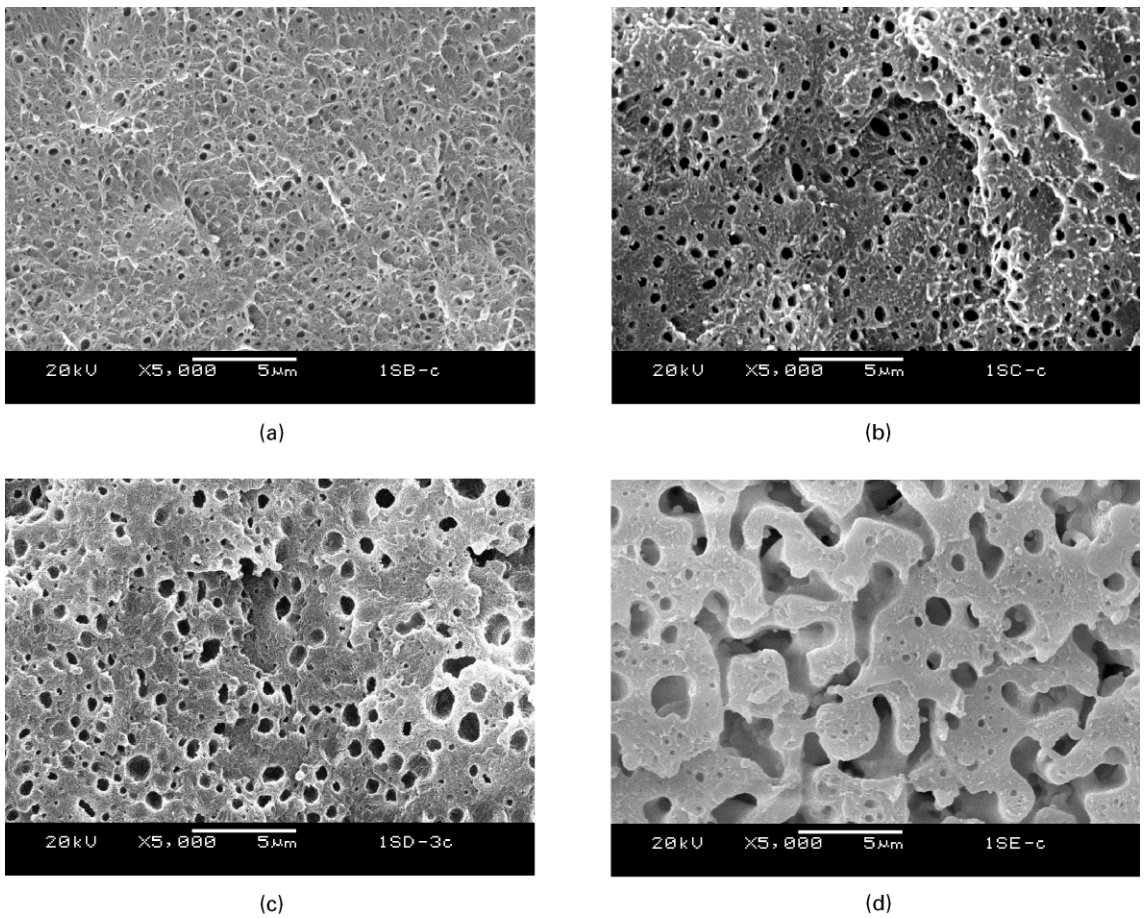

Fig. 1. The SEM photographs of static samples of HDPE/33EVA blends in the core. HDPE/33EVA: (a) 90/10; (b) 80/20; (c) 70/30; (d) 60/40.

2.4. Differential scanning calorimetry (DSC)

DSC measurements were performed on a Perkin–Elmer DSC priys-1 with both static sample and dynamic samples. The instrument was calibrated using indium as standard. Melting endotherms were obtained at 10 °C min^{-1} heating rate in 4–5 mg of sample in a nitrogen atmosphere. The degree of crystallinity was calculated from heat of fusion using 293 J g^{-1} as the heat of fusion of 100% crystalline HDPE [25].

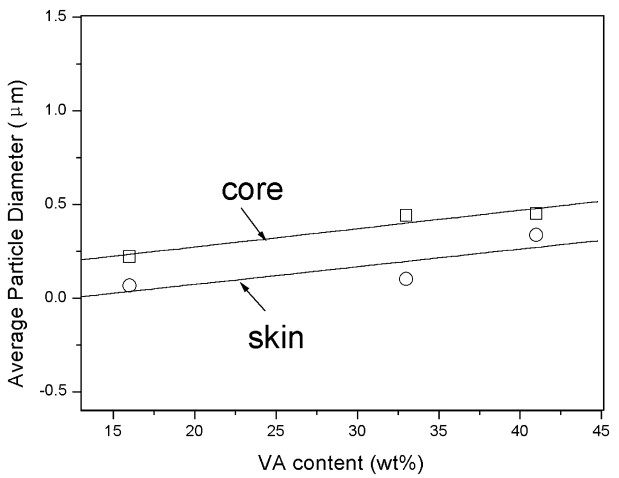

Fig. 2. The average particle diameter of static samples as a function of VA content, including skin layer and the core.

2.5. Scan electric microscope (SEM)

The phase morphology of HDPE/EVA blends was studied with the aid of an X-650 Hitachi scanning electron microscope Hitachi X-650 at 5 kV. The specimens were cryogenically fractured in liquid nitrogen and then the EVA phase is preferentially etched in benzene. The etching process was allowed to continue for 24 h at about 40 °C to reach the equilibrium condition. The solvent was removed from the specimen later using vacuum extraction. The surface was then coated with gold and subsequently examined.

3. Results

3.1. Phase morphology under the quiescent state

In HDPE/EVA blends, since the fast cooling of the melt at the surface of mold, usually the cross-section area of static sample can be divided into two parts: skin layer and

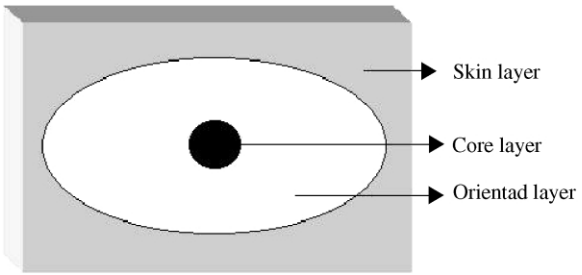

Fig. 3. The schematic representation of cross-section of specimen obtained by dynamic injection packing molding.

the core. The dispersed phase in the core has a bigger size than that in the skin layer, due to the temperature difference in the samples. The core has a higher temperature thus a longer time for phase separation. Shown as an example, Fig. 1 is the change of morphology of static sample of HDPE/33EVA at central part (the core) as a function of composition up to 40 wt% 33EVA. The black domains indicate the position of the extracted EVA phase. One observes a sea-island structure in the composition investigated, which indicates that EVA forms a dispersed phase and HDPE forms a continuous phase. The shape of EVA dispersed phase is spherical and the diameter of EVA increases from 0.4 to 1 μm when 33EVA content increases from 10 to 30 wt%. There is a big increase of EVA domain size (like a co-continuous structure) at 40 wt% EVA content. Similar results were found in HDPE/16EVA blends and HDPE/41EVA blends, but with different size of EVA. Fig. 2 shows the change of domain size of EVA as function of VA content for HDPE/EVA = 80/20. The sizes both in the skin layer and in the core are given in the figure. One finds an increase in EVA domain size with increase in VA content of EVA, from 0.06 to 0.33 μm in the skin layer, and from 0.22 to 0.45 μm in the core.

3.2. Phase morphology under low shear stress

In contrast to the static sample, macroscopically the shear-induced morphology of dynamic samples can be divided into three parts instead of two parts. As shown in Fig. 3, they are the core in the center and oriented zone surrounding the core and the skin layer. Fig. 4 shows the morphological change as a function of EVA content for HDPE/33EVA blends at the oriented zone where the effect of shear stress can be most demonstrated. Besides some spherical particles, the elongated and elliptical EVA particles are also observed. The size of dispersed EVA

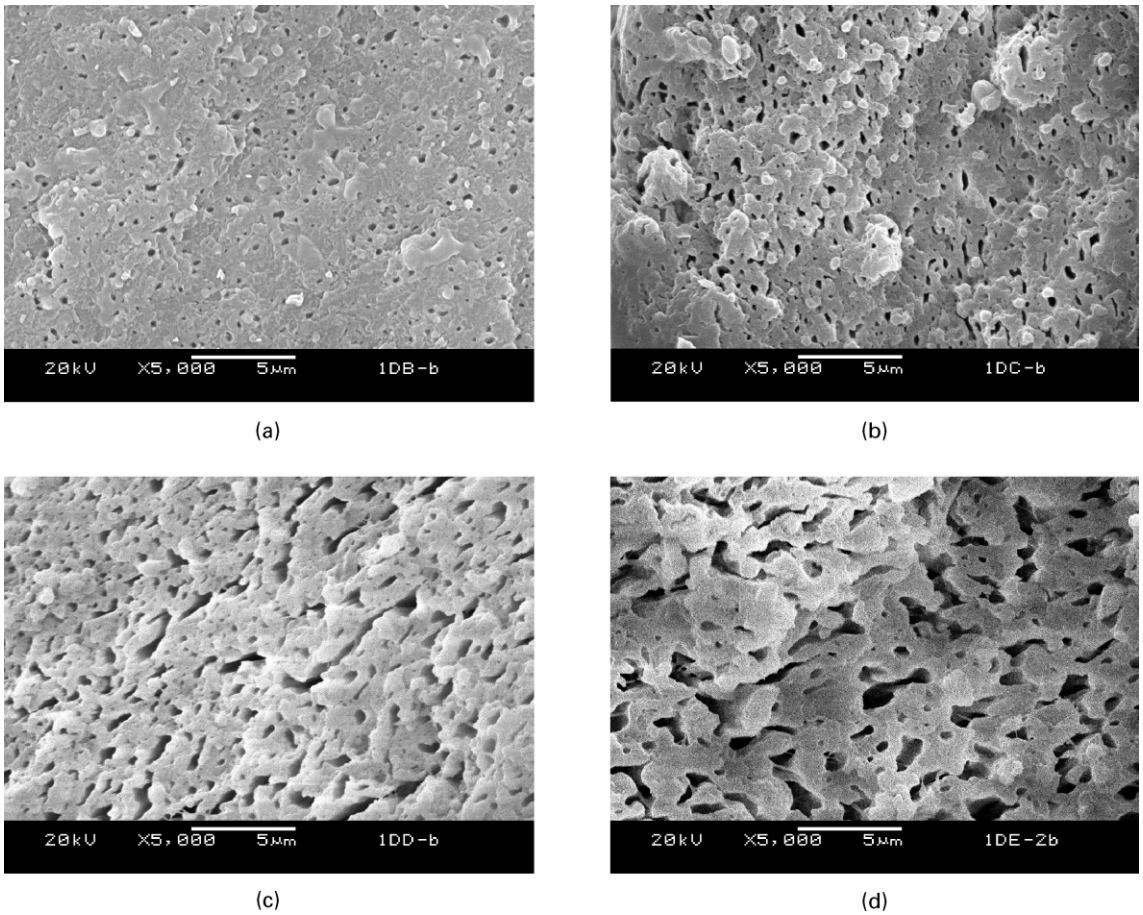

Fig. 4. The SEM photographs of dynamic samples of HDPE/33EVA blends in the oriented zone. HDPE/33EVA: (a) 90/10; (b) 80/20; (c) 70/30; (d) 60/40.

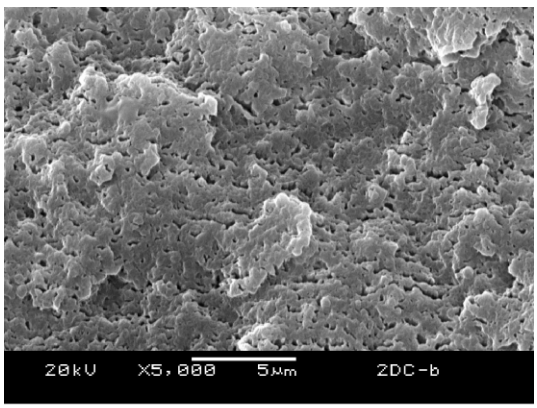

(a)

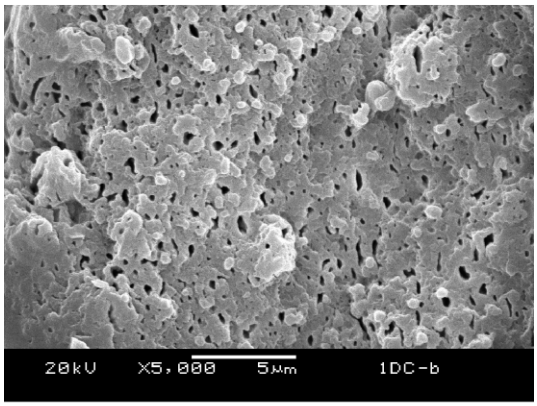

(b)

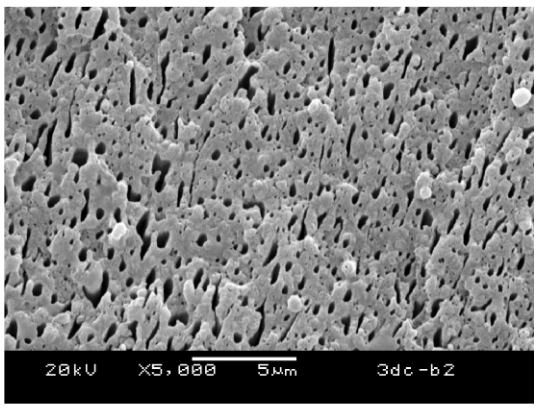

(c)

Fig. 5. The morphological changes of dynamic samples with the varying VA content in the oriented zone. (a) 16EVA; (b) 33EVA; (c) 41EVA.

domain also increases with increasing EVA content, and a somewhat co-continuous morphology is seen when EVA content reaches 30–40 wt%. Fig. 5 shows the morphological change as a function of VA content for HDPE/EVA = 80/20 at the oriented zone. One finds only a slight increase in EVA particle size with increase in VA content, more obvious change is the shape of EVA. In HDPE/41EVA, the highly oriented and elongated EVA particles are observed.

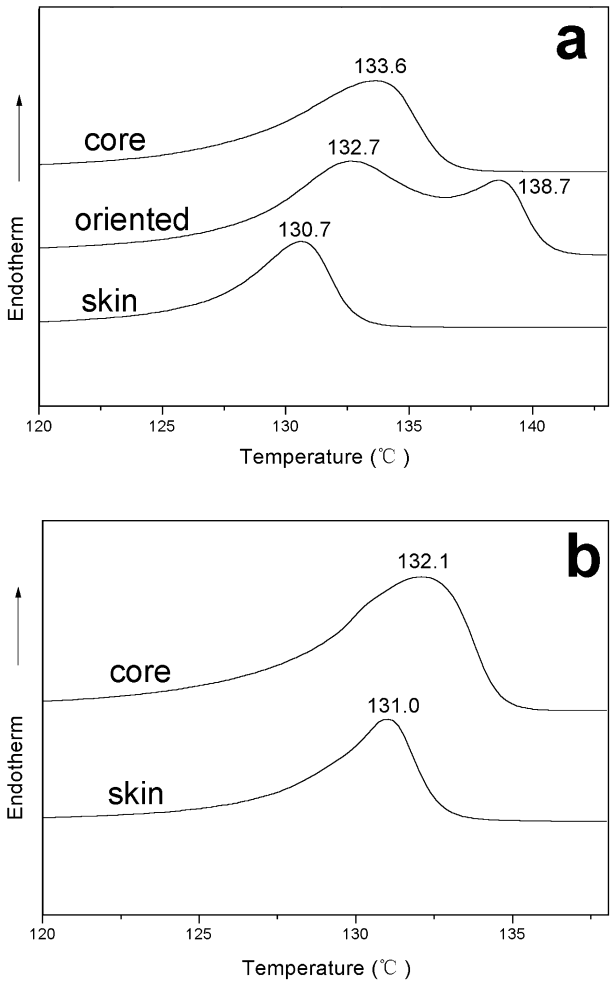

Fig. 6. DSC melting curves of HDPE/33EVA (80/20) blends: (a) dynamic samples and (b) static samples.

3.3. Melting behavior and crystallinity

The formation of different crystalline structures in shear stress field can also be demonstrated with the aid of DSC analysis. The slices used for DSC analysis is taken from different regions (skin, orientated and core layer) of the same sample, respectively. Showing as an example, Fig. 6 is the DSC heating curves of HDPE/33EVA = 80/20 obtained by both dynamic packing injection molding (Fig. 6a) and static packing injection molding (Fig. 6b). Only one peak can be observed in the melt curve of skin and core layer for both dynamic and static samples, which implies that in these two layers, only one crystal structure (most likely spherulite) exists and it may deform to some extent. However, in the oriented layer, two peaks appear in the melt curve of dynamic sample, which indicates that two crystal structures form, i.e. so-called shish kebab, as in the case reported by Bevis [18] The lower temperature peak is the melting of spherulites or lamellae of shish kebab, whereas the higher temperature peak is the melting of stretched chain of shish kebab. During the process of dynamic packing molding, the extension and orientation of

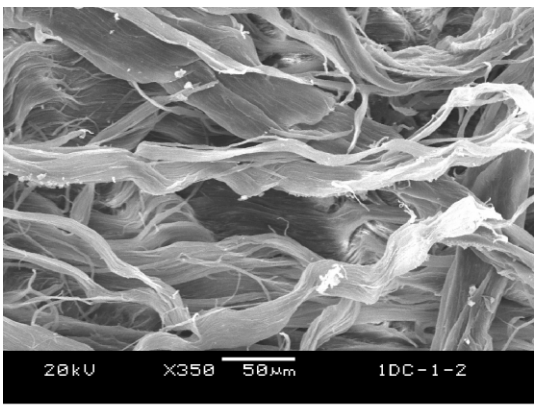

Fig. 7. The morphology of HDPE/33EVA (80/20) blends along flow direction in (a) low magnification and (b) high magnification.

the macromolecules is high at the melt/solid interface. This enhances the driving force for crystallization under a stressed state and raises the melting point, T_m, as well. The crystallization of the extended macromolecules of HDPE gives rise to formation of *c*-axis-crystallized fibers [18]. The unstretched portions of extended HDPE chains

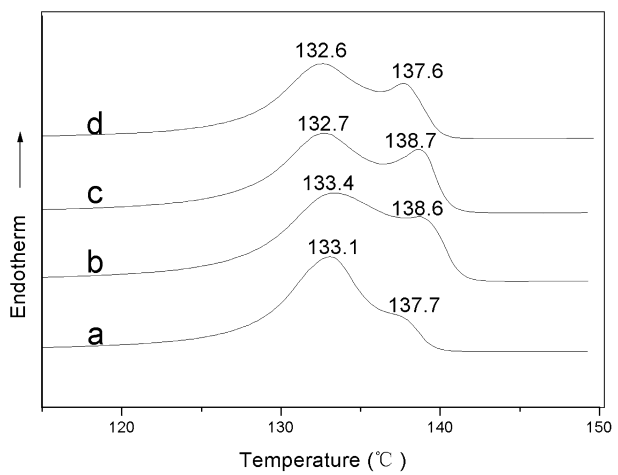

Fig. 8. DSC melting curves of pure HDPE and HDPE/EVA (80/20) blends with varying VA content in the oriented zone. (a) Pure HDPE; (b) 16EVA; (c) 33EVA; (d) 41EVA.

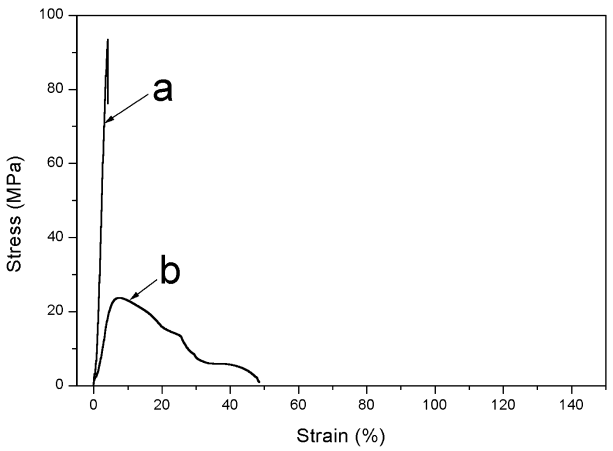

Fig. 9. The stress–strain curve of HDPE/16EVA blends: (a) dynamic sample and (b) static sample.

crystallize in the form of chain-folded lamellae [9], which in combination with the fibers previously crystallized, form a so-called shish kebab structure. The fibrillar structure of oriented sample of HDPE/33EVA = 80/20 is shown in Fig. 7 as an example. The SEM photographs were taken along the flow direction. One observes the HDPE fibers at low magnification (Fig. 7a) and highly oriented and elongated EVA domains at high magnification (Fig. 7b). The melting

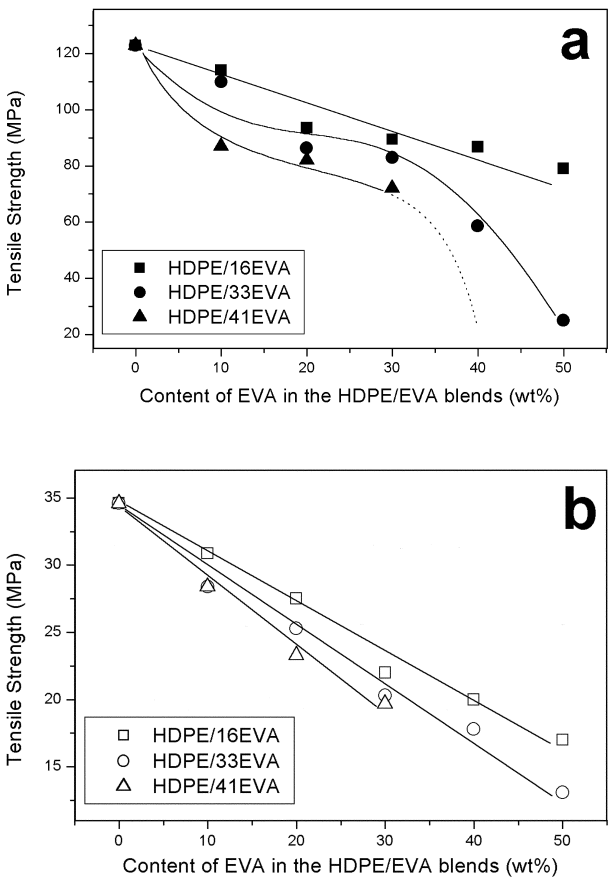

Fig. 10. The tensile strength of HDPE/EVA blends as a function of composition: (a) dynamic samples and (b) static samples.

Table 3
Values of melt point and crystallinity of HDPE/16EVA blends

Code		Melt point (°C)						Crystallinity (%)		
		100/0		90/10		80/20		100/0	90/10	80/20
		First peak	Second peak	First peak	Second peak	First peak	Second peak			
Dynamic samples	Skin layer	131.6	–	131.2	–	131.3	–	49.9	54.1	52.1
	Oriented layer	133.1	137.7	132.5	138.4	133.4	138.6	56.6	57.7	63.9
	Core layer	133.4	–	133.0	–	132.2	–	60.3	55.4	58.4
Static samples	Skin layer	131.5	–	130.4	–	131.3	–	51.2	46.8	48.0
	Core layer	133.7	–	132.2	–	132.5	–	55.6	50.8	54.1

curves of oriented layer of HDPE/EVA = 80/20 with different VA contents are shown in Fig. 8. The intensity of high temperature peak is seem to increase by adding EVA compared with pure HDPE, which indicates that presence of EVA can promote the formation of stretched chain. However, the VA content in EVA has no apparent effect on the melting behavior of oriented layer. The melt point and crystallinity of HDPE/16EVA and HDPE/33EVA blends are listed in Tables 3 and 4. The crystallinity is obtained according to the equation

$$\text{crystallinity} = \frac{\Delta H_f}{\Delta H_f^m \cdot \chi_A} \times 100\% \quad (1)$$

where ΔH_f is the enthalpy of HDPE in the blends, ΔH_f^m is the enthalpy of HDPE whose crystallinity is 100%, the value is 293 J g^{-1}, and χ_A is the content of HDPE in the blends. For both the dynamic and static sample, the crystallinity of core layer is higher than that of skin because the degree of perfection of lamellae is poor in the skin layer as a result of fast frozen. On the other hand, the crystallinity of oriented layer is higher than that of core and skin layer. This can be well explained by shear-induced crystallization of HDPE during dynamic packing injection molding.

3.4. Mechanical properties

Fig. 9 shows the typical stress–strain curves of specimens prepared by dynamic packing and static packing. The dynamic specimen breaks in a brittle manner (elongation is less than 10%), whereas the static specimen is ductile. The tensile strengths of HDPE/EVA blends obtained by both static and dynamic packing injection molding are shown in Fig. 10 as a function of composition. One finds almost a linear decrease in tensile strength with increase in EVA content for the static sample, as expected. The VA content in EVA does not have very much effect on the tensile strength of HDPE, which changes from 34 to 12–17 MPa as EVA content increase to 50 wt% for all the three kinds of EVA. On the other hand, for the dynamic sample, the tensile strength of pure HDPE is greatly enhanced to 125 MPa. For the blends, the tensile strength declines to 70–90 MPa as increasing of EVA content to 30 wt%. For HDPE/16EVA, a linear relationship is seen up to 50 wt% 16EVA. However, one observes a sharp drop of tensile strength at 30 wt% for HDPE/33EVA and HDPE/41EVA blends. Young's modulus of the dynamic samples is much higher than that of static samples as a result of shear induced-molecular orientation. This is listed in Table 5. For example, the modulus of HDPE is 0.71 GPa for static sample, but 2.47 GPa for dynamic sample; for the blends of HDPE/EVA = 80/20, 0.48–0.52 GPa for the static samples, while 1.77–2.17 GPa for the dynamic samples. Moreover, the tendency of modulus varying with the composition (both dynamic and static) is same as that of tensile strength.

The enhancement of tensile strength and modulus mostly originated from the formation of oriented layer that consists of microfibers in the dynamic samples. Consequently, with the increasing EVA content, the amount of molecules

Table 4
Values of melt point and crystallinity of HDPE/33EVA blends

	Melt point (°C)						Crystallinity (%)		
	100/0		90/10		80/20		100/0	90/10	80/20
	First peak	Second peak	First peak	Second peak	First peak	Second peak			
Dynamic samples	Skin layer	131.6	–	132.0	–	130.7	–	49.9	54.6	52.7
	Oriented layer	133.1	137.7	133.2	138.5	132.7	138.7	56.6	59.6	60.7
	Core layer	133.4	–	133.3	–	133.6	–	60.3	58.3	56.2
Static samples	Skin layer	131.5	–	132.4	–	131.0	–	51.2	50.7	49.3
	Core layer	133.7	–	132.8	–	132.1	–	55.6	56.4	54.3

Table 5
Values of Young's modulus (GPa) of HDPE/EVA blends

	100/0	90/10	80/20	70/30	60/40	50/50	
HDPE/16EVA	Oscillating	2.47	2.39	2.17	2.01	1.85	1.55
	Static	0.71	0.65	0.49	0.46	0.42	0.36
HDPE/33EVA	Oscillating	2.47	2.31	1.86	1.81	1.41	0.56
	Static	0.71	0.59	0.52	0.41	0.36	0.26
HDPE/41EVA	Oscillating	2.47	1.84	1.77	1.51	–	–
	Static	0.71	0.59	0.48	0.39	–	–

forming microfibers decreases, thus the tensile strength declines with the arising of EVA content in HDPE/EVA (either 16EVA, 33EVA or 41EVA). In addition, the amount of orientation structure that depends on rheological properties, melt temperature, die temperature as well as dynamic frequency and pressure plays a vital role for the tensile strength [16]. Fig. 11 shows the corresponding relative impact strength of HDPE/EVA blends produced by static and dynamic packing injection molding. The impact strength of static specimen in general rises with increasing of the content of EVA, which is in agreement with the classic theory [7]. For the dynamic specimens, one observes

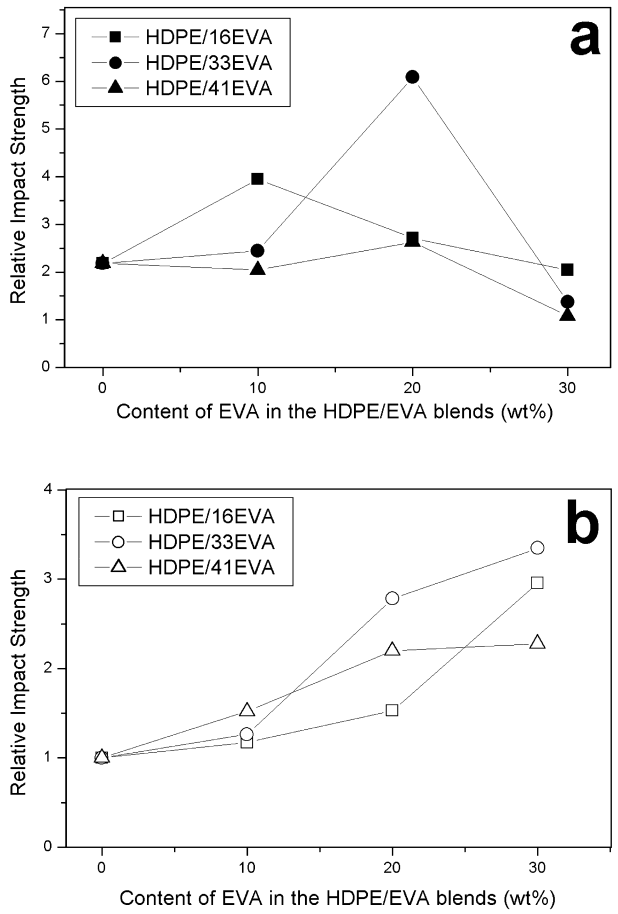

Fig. 11. The relative impact strength of HDPE/EVA blends as a function of composition, taking the value of pure HDPE of static sample as 1: (a) dynamic samples and (b) static samples.

a maximum at 10 wt% EVA for HDPE/16EVA, and at 20 wt% EVA for HDPE/33EVA and HDPE/41EVA. At the maximum of HDPE/33EVA, a six times increase of impact strength is achieved compared with the static sample of pure HDPE.

Therefore, it can be concluded that super HDPE/EVA blends having high modulus (1.9–2.2 GPa), high tensile strength (100–120 MPa) and high impact strength (six times as that of pure HDPE) can be obtained by controlling the phase separation, molecular orientation and crystal morphology of the blends via dynamic packing injection molding.

4. Discussion

4.1. Miscibility and mechanical properties

Thermodynamically, the polymer–polymer interaction parameter, χ_{12}, is one of the key parameters to determine the miscibility of polymer blends. It can be calculated by

$$\chi_{12} = \frac{V_r(\delta_1 - \delta_2)^2}{RT} \tag{2}$$

where δ_i are the solubility parameters of the two homopolymers or copolymers, R is the gas constant, T is the absolute temperature, and V_r is the reference volume, taken as 100 cm^3 for polymers. For HDPE/EVA blends, Krause calculated the χ_{12} as changing of VA content of EVA by using Hildebrand solubility parameters [26]. The Hildebrand solubility parameters of the homopolymers were calculated using

$$\delta = \frac{\rho \sum F_i}{M} \tag{3}$$

where δ is the solubility parameter of the polymer, $\sum F_i$ is the sum of the molar attraction constants of all the groups in the repeat group of the polymer. M is the molecular weight of the repeat group, and ρ is the density of the polymer at given temperature. While for random copolymer, the solubility parameters can be calculated using

$$\delta_c = \sum \delta_i \phi_i \tag{4}$$

where δ_c is the solubility parameter of the copolymer, δ_i is the solubility parameter of the homopolymer corresponding to repeat group i, and ϕ_i is the volume fraction of repeat group i in the copolymer.

For our HDPE/EVA blends, the calculated interaction parameters at 25 and 180 °C are listed in Table 6. The densities at 25 and 180 °C for polyethylene were taken as 0.965 and 0.785 g cm^{-3}, and 1.19 and 1.00, respectively, for EVA. One finds a great increase of χ_{12} as VA content changes from 16 to 41 wt% in EVA. By comparing χ_{12} with the so-called calculated critical interaction parameter, Krause predicted that EVA may be completely miscible with HDPE molecules when EVA contains less than 18 wt%

Table 6
Calculated interaction parameter for mixtures of the different copolymer with polyethylene

Copolymer	χ	
	25 °C	180 °C
16EVA	0.12	0.088
33EVA	0.56	0.40
41EVA	0.90	0.64

VA, even for a high molecular weight average of 10^5 of HDPE and EVA [27]. So for our system, HDPE/16EVA blends can be considered phase miscible in the melt state (180 °C) but subject to phase separation after crystallization of HDPE at low temperature. On the other hand, for HDPE/33EVA and HDPE/41EVA blends, they are most likely phase separated even in the melt state. Phase behavior affects not only the domain size of EVA in HDPE matrix, which increases with increase in VA content, but also the mechanical properties of both static and dynamic samples. As shown in Fig. 10 and Table 5, the good interaction between HDPE and EVA is very helpful for enhancement of tensile strength and modulus of the blends. However, for impact strength, a suitable interaction is needed for the best enhancement. As shown in Fig. 11, completely miscible or macroscopic phase separation only results in limited reinforcement of impact strength of HDPE/EVA blends. The highest impact strength is seen for HDPE/33EVA blends which have an inter-middle interaction parameter in the studied system.

4.2. Impact strength vs. the shape of dispersed particles

One of the most important findings in polymer-toughening is the so-called critical matrix ligament thickness (T_c) theory, which is developed by Wu after an investigation on Nylon 6/EPDM blends [7,8]. It is proposed that T_c is the only parameter to determine the brittle–ductile (B–D) transition of the blends. Only when the matrix ligament thickness (T) is smaller than T_c can the shear yielding of matrix ligament exist and B–D transition of blends occurs. More than 10 times increase of impact strength was observed for Nylon 6/EPDM blends at the B–D transition. For given blends, T_c is independent of the volume fractions and particle size of the rubber. The theory, which has also created much controversy, has been further clarified by Muratoglu et al. [28] who have proposed that the incoherent particle–matrix interfaces stimulate a preferential form of crystallization over a definite distance around the particles with the lowest energy surfaces of crystalline lamellae representing also the crystallographic planes of lowest plastic resistance lying parallel to the interfaces, and furthermore, the Wu's theory has a prerequisite: the rubber particles are considered as cubic or spherical and randomly distributed in the matrix. If the rubber particles are elongated and oriented, the stress field around a particle will not be homogeneous anymore. The more stress concentration will be expected at the tip than at the other directions. The brittle–ductile–brittle transition has been reported in PP/EPDM blends obtained by dynamic packing injection molding as increasing of EPDM content [29]. Here once again, as shown in Fig. 11a, for HDPE/EVA blends, particularly for HDPE/33EVA blends, one observes a clear-cut brittle–ductile–brittle transition of impact strength as increasing of EVA content. Our result indicates clearly that the Wu's theory cannot apply to the elongated and oriented rubber particles. It is not clear at this moment how and why the observed brittle–ductile–brittle transition takes place, but certainly results from the orientation and elongation of dispersed particles caused by shear stress. The particle–matrix interfaces also play a very important role, as we see a strong transition in HDPE/33EVA blends and a weak transition in HDPE/41EVA blends, HDPE/16EVA blend lies in between. Since the fracture direction also plays role to determine the impact strength, further fracture experiments are needed on samples containing EVA particles with different orientation with respect to the fracture propagation direction. This work is undertaken by our group.

4.3. Region of phase inversion

The phase inversion is a common phenomenon in immiscible polymer blends. Jordhamo et al. [30] developed an empirical model based on the melt-viscosity ratio, η_d/η_m, and the volume fraction ϕ, of each phase for predicting the phase inversion region in immiscible polymer blends. Phase inversion should take place as the following criterion holds:

$$\frac{\eta_1}{\eta_2}\frac{\phi_2}{\phi_1} = 1 \tag{5}$$

Jordhamo's model however is limited to low shear rates and does not take into account the effect of variations in the interfacial tension between the phases. For the HDPE/EVA blends studied here, both the shear stress and interfacial tension should be considered to explain the observed region of phase inversion. As mentioned earlier, HDPE/16EVA blends most likely form a homogeneous phase in the melt state. One may not expect to see any phase inversion in this system. However, HDPE/33EVA and HDPE/41EVA should belong to immiscible polymer blends based on the calculated interaction parameters, thus the region of phase inversion should exist. Due to the difficulty of sample preparation, in our work the content of EVA was limited to 50 wt% for 33EVA and 30 wt% for 41EVA. Since the viscosity ratio during processing conditions is not available at moment, one cannot predict the region of phase inversion. For HDPE/33EVA blends, it should be around 40 wt% EVA content from the SEM results of static samples (Fig. 1). Correspondingly, one sees a linear decrease of tensile strength as increasing of EVA content up to 50 wt% (Fig.

10b). For dynamic samples, however, the phase inversion is found around 30–40 wt% EVA contents, and a co-continuous phase is observed. This is shown in Fig. 4, which indicates that the region of co-continuity shifts towards lower EVA content under shear stress filed. Correspondingly, a sharp decrease of tensile strength at 30 wt% content is seen for dynamic samples (Fig. 10a).

5. Conclusion

The super HDPE/EVA blends having high modulus (1.9–2.2 GPa), high tensile strength (100–120 MPa) and high impact strength (six times as that of pure HDPE) have been prepared by controlling the phase separation, molecular orientation and crystal morphology of the blends via dynamic packing injection molding. Interfacial interaction between HDPE and EVA plays an important role to determine the phase morphology (size and shape) and thus mechanical properties. The phase inversion was found to shift towards lower EVA content under shear stress. The increase of tensile strength and modulus is due to the formation of oriented zone where shish kebab crystal structure is induced under shear. While the enhancement of impact strength is caused by oriented and elongated EVA particles, a brittle–ductile–brittle transition was observed. This result indicates that Wu's theory is no longer valid for oriented and elongated particles.

Acknowledgements

We would like to express our great thanks to the China National Distinguished Young Investigator Fund and National Science Foundation of China for financial support.

References

[1] Utracki LA. Polymer alloys and blends: thermodynamics and rheology. New York: Hanser; 1989.
[2] Nomura T, Nishio, et al. J Appl Polym Sci 1995;55:1307.
[3] Cieslinski RC, Silvis HC, Murry DJ. Polymer 1995;36:1827.
[4] Yokoyama Y, Ricco T. Polymer 1998;39:3675.
[5] Wangmer GJ. Soc Plast Engng RTTEC Polyolefins 1993;8:539.
[6] Borggreve, et al. Polymer 1987;28:1489.
[7] Margolina A, Wu S. Polymer 1988;29:2170.
[8] Wu S. J Appl Polym Sci 1988;35:549.
[9] Keller A. Polymer 1962;3:293.
[10] Ward IM, Wilding MA. J Polym Sci, Polym Phys Ed 1984;22:561.
[11] Coates PD, Ward IM. Polymer 1979;20:1553.
[12] Gibson AG, Ward IM. J Polym Sci, Polym Phys Ed 1978;16:2015.
[13] Hine PJ, Ward IM, Olley RH, Basset DC. J Mater Sci 1993;28:316.
[14] Odell JA, Grubb DT, Keller A. Polymer 1978;19:617.
[15] Kubát J, Mánson J-A. Polym Engng Sci 1983;23:869.
[16] Guan Q, Shen K, Ji J, Zhu J. J Appl Polym Sci 1995;55:1797.
[17] Ogbonna CI, Kalay G, Allan PS, Bevis MJ. J Appl Polym Sci 1995;58:2131.
[18] Kalay G, Sousa RA, Reis RL, Cunha AM, Bevis MJ. J Appl Polym Sci 1999;73:2473.
[19] Zhang G. PhD Thesis. Sichuan University, Chengdu, China; 2000.
[20] Wang Y, Zou H, Fu Q. J Appl Polym Sci 2002; in press.
[21] Beger W, Kammer HW, Kummerlowe C. Macromol Chem Suppl 1984;8:01.
[22] Karger Kocsis J, Csikai I. Polym Engng Sci 1987;27:241.
[23] VanOene H. J Colloid Interf Sci 1972;40:448.
[24] Ray I, Khastgir D. Polymer 1993;34:2030.
[25] Wunderlich B. Thermal analysis. New York: Academic Press; 1990.
[26] Krause S. In: Paul DR, Newman S, editors. Polymer blends. New York: Academic Press; 1978.
[27] Ruth L, et al. Macromolecules 1996;29:4258.
[28] Muratoglu OK, Argon AS, Cohen RE, Weinberg M. Polymer 1995;36:4787.
[29] Wang Y, Li Q, Fu Q. Macromol Engng Mater 2002;287:391.
[30] Jordhamo GM, Manson JA, Sperling LH. Polym Engng Sci 1986;26:517.